



**HAL**  
open science

# Compaction of liquid immersed granular packings by small upward flows

Georges Gauthier, Philippe Gondret

► **To cite this version:**

Georges Gauthier, Philippe Gondret. Compaction of liquid immersed granular packings by small upward flows. *Physical Review Fluids*, 2019, 4 (7), pp.074308. 10.1103/PhysRevFluids.4.074308 . hal-03898550

**HAL Id: hal-03898550**

**<https://hal.science/hal-03898550>**

Submitted on 10 Mar 2024

**HAL** is a multi-disciplinary open access archive for the deposit and dissemination of scientific research documents, whether they are published or not. The documents may come from teaching and research institutions in France or abroad, or from public or private research centers.

L'archive ouverte pluridisciplinaire **HAL**, est destinée au dépôt et à la diffusion de documents scientifiques de niveau recherche, publiés ou non, émanant des établissements d'enseignement et de recherche français ou étrangers, des laboratoires publics ou privés.

# Compaction of liquid immersed granular packings by small upward flows

Georges Gauthier and Philippe Gondret<sup>1</sup>

<sup>1</sup>*Laboratoire FAST, Univ. Paris-Sud, CNRS, Université Paris-Saclay, F-91405, Orsay, France.*

We study experimentally the compaction dynamics of a fully-immersed granular packing subjected to a slow upward flow. We consider continuous flows as well as discontinuous flows featuring short flow bursts that act as flow “taps”. We monitor the compaction rate of initial packings prepared by settling, and find that compaction is possible for a continuous flow with upward velocities below the fluidization threshold. Flow bursts are found strongly to enhance the compaction efficiency, especially when the bursts are above the fluidization threshold.

## I. INTRODUCTION.

How identical spheres arrange in a dense packing is a long standing scientific question that aroused many fundamental works since the famous Kepler conjecture: even if the solid fraction in the tetrahedral arrangement of four equal spheres in contact is 0.78, the highest solid fraction that can be achieved in a large packing is 0.74. This value corresponds to the densest periodic arrangement of equal spheres. In contrast, disordered packings correspond to much lower solid fractions. Random packings of equal spheres have a solid fraction of about 0.6 with a Random Loose Packing limit (RLP) of about 0.56 and a Random Close Packing (RCP) of about 0.64. For granular systems that are athermal and dissipative, the exploration of the different possible arrangements cannot be driven by temperature and must be driven by an external input of mechanical energy. This can be achieved by different modes of loading. The most classical way of compaction is the mechanical shaking of the container by successive taps [1–6] or harmonic vibrations [7]. The solid fraction first sharply increases, and then keep increasing but more slowly toward a plateau. Two main empirical laws are used for describing the time evolution of the solid fraction from the initial packing value  $\phi_0$  to the final one  $\phi_\infty$ . The first law is expressed using a logarithmic time dependence, as [1, 2]:

$$\frac{\phi(t) - \phi_0}{\phi_\infty - \phi_0} = 1 - \frac{1}{1 + B \ln(1 + t/\tau)}, \quad (1)$$

where  $\tau$  is a characteristic time of the compaction dynamics and the parameter  $B$  is related to the compaction efficiency. The second law involve an exponential time dependence, as [1, 3–5]:

$$\frac{\phi(t) - \phi_0}{\phi_\infty - \phi_0} = 1 - e^{(-t/\tau)^\beta}, \quad (2)$$

involving a characteristic time  $\tau$  and an exponent  $\beta$  related to the compaction efficiency.

The logarithmic evolution of Eq. (1) may be explained from simple theoretical arguments [8, 9], e.g. by considering the process where a grain can jump into a hole only if the hole is large enough and by considering a distribution of hole sizes of Poisson type with a characteristic free volume [8]. The stretched exponential law is frequently

used in a large range of relaxations of disordered thermal systems such as glasses [3]. The logarithmic evolution is experimentally observed for “confined” packings where the container-to-grain size ratio  $D/2a$  is not very large ( $D/2a \lesssim 10$ ), whereas the stretched exponential is observed for “unconfined” packings ( $D/2a \gtrsim 10$ ). In the tapping experiments of monodisperse spheres, the solid packing fraction typically increases from  $\phi_0 \simeq 0.58$  to  $0.61 \lesssim \phi_\infty \lesssim 0.63$ . The characteristic time  $\tau$  decreases with increasing level of vibrations so that compaction is quicker for larger vibrations. By contrast, the final solid fraction  $\phi_\infty$  decreases with increasing level of vibrations so that compaction is higher for smaller vibrations [2, 3]. Thus, an optimal way of compaction is to apply first large vibration levels for a first quick compaction before low vibration levels to achieve a final higher compaction up to about  $\phi_\infty \simeq 0.65$ .

Compaction has been shown to be also possible by shearing the granular packing from lateral wall deformation (e.g. [10, 11]). This process appears to be quite efficient, with compaction ranging from  $\phi_0 \simeq 0.59$  up to  $0.66 \lesssim \phi_\infty \lesssim 0.69$  depending on the shear amplitude after a few  $10^4$  cycles typically. Such high values of solid fraction are beyond the RCP limit and ordering is observed with some crystalline clusters at the walls but also in the bulk. In these shearing experiments, the compaction dynamics is complex and does not follow any of the model equations (1-2) mentioned above.

When grains are cohesive, the observed packing fractions are much lower, with reported values as low as 0.1, and display some compaction under vibrations by a two stage process with two timescales, a short one and a large one, which are associated to collective and individual grain motions [12].

When the grains are fully immersed into a liquid, the bed packing that arises from settling depends on the hydrodynamic forces that come into play, which themselves depend on the particle Reynolds number and Stokes number [13, 14], that compare fluid inertia and particle inertia, respectively, to viscous dissipation. Using fluidization/sedimentation cycles Schröter *et al.*[15] studied the fluctuation statistics of the solid fraction of the obtained bed packings which display small relative variations of about 0.1%. As for dry packings, compaction of liquid immersed granular packings can be achieved by taps [16] or harmonics vibrations [17]. In these compaction exper-

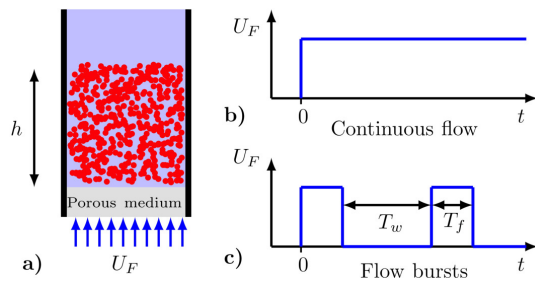


FIG. 1. (a) Sketch of the experimental set-up. (b) Continuous flow with the constant upward velocity  $U_F \neq 0$ . (c) Bursting flow with the time period  $T = T_w + T_f$  made of successive flow time  $T_f$  separated by non flow time  $T_w$ .

iments where glass beads of about half a millimeter in diameter are immersed in a viscous liquid from one time to one thousand times the viscosity of water, the frequency is about the same ( $\sim 50$  Hz) and the maximal acceleration is about the same ( $\sim 10g$ , where  $g$  is the gravity acceleration), but the oscillation amplitudes are smaller than the grain size [17] whereas the tap amplitudes are larger than the grain size [16]. The solid fraction is observed to increase from about  $\phi_0 \simeq 0.57$  [16] or  $0.58$  [17] up to  $0.60 \lesssim \phi_\infty \lesssim 0.62$  [17] or  $0.64 \lesssim \phi_\infty \lesssim 0.65$  [16], but the compaction dynamics is however more complex than in the dry case and cannot be given by the previous model equations (1-2). Indeed, a first quick dynamics followed by a second slow dynamics are observed and the resulting dynamics has to be fitted by either a change in the exponent  $\beta$  of Eq. (2) [17] or by a change in the parameter  $B$  of Eq. (1) [16].

Despite all the previous reported studies, the compaction dynamics of granular packings is not fully understood. Yet the solid fraction of granular packings is a key parameter in numerous phenomena such as avalanches [18, 19], impact cratering [20] or animal locomotion [21]. In some of these recent experiments, either air flow pulses [21] or a combination of continuous air flow and vibrations [19] are used to generate different compaction states.

In the present paper, we look at the possible compaction of liquid immersed granular packings by upward flows which are either continuous or discontinuous with short flow bursts that act as flow “taps”. In section II, we present the experimental set-up that allow to prepare the initial packing from the settling of a fluidized bed before applying the upward flow. Then we show results for the compaction dynamics of the packing when submitted to a continuous flow below the fluidization threshold in section III, and to successive short flow bursts in section IV.

## II. EXPERIMENTAL SET-UP

The experimental set-up is sketched in Fig. 1. Glass beads of radius  $a = (1 \pm 0.05)$  mm and density  $\rho_p = 2.3 \times 10^3$  kg/m<sup>3</sup> are dispersed in a water-glycerol mixture of 90% in mass of glycerol, with thus a density  $\rho = 1235 \pm 1$  kg/m<sup>3</sup> and viscosity  $\eta = (0.156 \pm 0.012)$  Pa · s at  $(24 \pm 1)$  °C. For the whole set of experiments, the total mass  $M_p$  of particles has been kept constant with the value  $M_p = 360 \pm 0.01$  g. The liquid immersed beads are contained in a vertical parallelepipedic cell of 50 cm high and of rectangular cross-section  $S = 8 \times 2$  cm<sup>2</sup>. The liquid is injected through a 2 cm high porous medium located at the bottom of the cell and fitted with its rectangular section. The porous medium opening is  $50 \mu\text{m}$ , with a permeability which is two orders of magnitude lower than the permeability of the granular bed. The upward volume flow rate  $Q$  is fixed using a gear pump allowing fluid circulation without any significant noise and dependence to pressure loss which mainly comes from the porous media. The pump is controlled with a wave form generator which allows any requisite flow variations. For periodic bursts, we have checked that the flow rate in the cell is the one set, with no overshoot and very short time rise (smaller than  $1/15$  s) when the flow is turned on, and the same very quick response when the flow is turned off. We do not observe any mechanical disturbance when the flow is turned on or off. The experimental tank is lightened from behind and images of the cell are taken at the maximum rate of 15 images per second thanks to a camera located 1 meter from the cell and with its axis horizontal and perpendicular to the largest side of the cell. The global solid volume fraction of the bed is measured through image analysis. From each individual image taken at time  $t$ , the bed surface is tracked and averaged spatially to obtain the mean instantaneous height  $h(t)$  of the bed. We do not observe any significant curvature of the bed surface across the width and the thickness of the cell, but a flat profile. The mean solid volume fraction  $\phi(t)$  of the bed at time  $t$  is then deduced from  $h(t)$  as  $\phi(t) = M_p / \rho_p S h(t)$ , with an accuracy  $\delta\phi/\phi = \delta h/h \simeq 10^{-3}$ . Indeed in our experiments, the initial height value of the packing is about  $h_0 \simeq 16$  cm for  $\phi_0 \simeq 0.6$  and the accuracy of its measurement is  $\delta h \simeq 0.1$  mm.

Considering the particles and the fluid used, the typical settling velocity of one isolated spherical particle is expected to be given by the Stokes velocity  $U_s = 2(\rho_p - \rho)ga^2/9\eta \simeq 15$  mm/s corresponding to a viscous regime with a low particulate Reynolds  $Re_p = \rho U_s a / \eta \simeq 0.1$ . The Stokes number corresponding to the ratio of particle inertia to viscous dissipation is  $St = 2\rho_p U_s a / 9\eta \simeq 0.05$ , thus very far below the critical value  $St_c \simeq 10$  corresponding to the bouncing transition [22, 23]. This means that all kinetic energy is dissipated in the fluid in the grain contact process. In a low  $Re$  fluidized bed, the solid volume fraction  $\phi$  is imposed by the upward flow velocity  $U_F = Q/S$  according to the Richardson-

Zaki law (RZ in the following) which reads [24, 25] :  $\phi = 1 - (U_F/U_s)^{1/n}$ . As shown in Fig. 2, our experimental data  $\phi(U_F)$  agree fairly well with the RZ law with the exponent value  $n \simeq 4.2$  and the experimental Stokes velocity  $U_s \simeq 16$  mm/s close to the previously estimated value for a perfect monodisperse suspension of spheres.

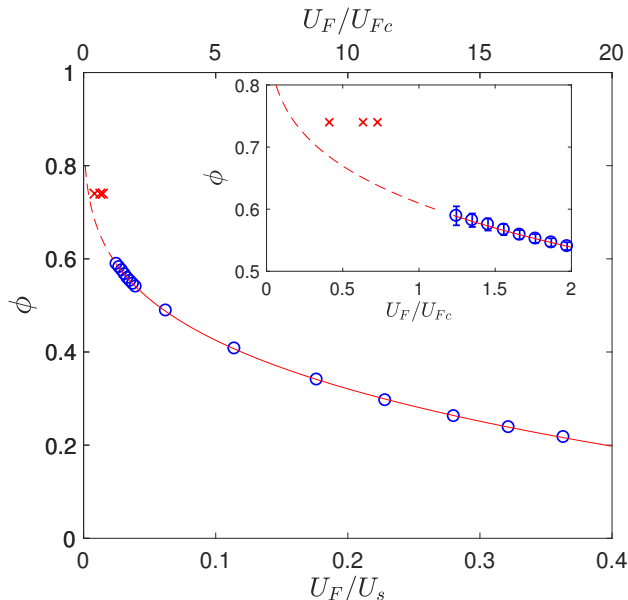


FIG. 2. Solid fraction of the granular bed  $\phi$  as a function of the upward fluid velocity  $U_F$  normalized by the Stokes velocity  $U_s$  (bottom axis) or the critical fluidization velocity  $U_{Fc}$  (top axis). (○) Experimental data for fluidized beds above the fluidization threshold  $U_{Fc}/U_s = 0.02$  and (—) best fit by RZ law  $\phi = 1 - (U_F/U_s)^{1/n}$  with  $n \simeq 4.2$  and  $U_s \simeq 16$  mm/s. (×) Final value  $\phi_\infty$  from best fit by Eq. (1) of  $\phi(t)$  data of Fig. 3 corresponding to compaction experiments at  $U_F < U_{Fc}$ . Inset: Zoom on flow range  $U_F/U_{Fc} \leq 2$ .

Each initial granular pile is prepared following the same procedure. First, a fluidized suspension of solid fraction  $\phi \simeq 0.22$  is obtained by imposing a constant upward velocity  $U_F \simeq 5.7$  mm/s  $\simeq 0.35U_s$ . Then the upward flow is switched off and the suspension settles achieving a granular pile of solid fraction  $\phi_0 = 0.605 \pm 0.005$ . The critical fluidization velocity deduced from the RZ law for beds of initial packing fraction  $\phi_0 = 0.605 \pm 0.005$  is  $U_{Fc} \simeq (0.02 \pm 0.001)U_s$ . For  $U_F > U_{Fc}$ , the granular pile expands again towards a fluidized suspension of solid fraction  $\phi < \phi_0$  according to the RZ law. In the following, we present experimental results for the compaction dynamics of the initial packing resulting from either a continuous flow (Fig. 1b) below the fluidization threshold ( $U_F < U_{Fc}$ ) or successive flow bursts (Fig. 1c).

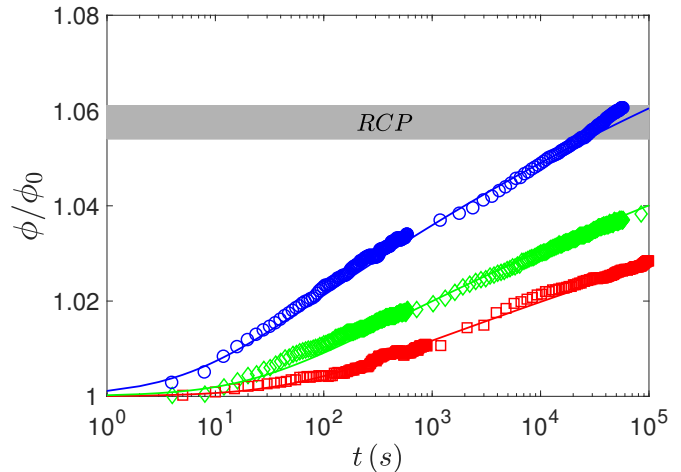


FIG. 3. Time evolution of the normalized solid fraction  $\phi/\phi_0$  of the packing submitted to an upward continuous flow at three different velocities  $U_F/U_{Fc} = 0.4$  (□),  $0.6$  (◇) and  $0.7$  (○) from an initial packing fraction  $\phi_0 = 0.606$  (□),  $0.607$  (◇), and  $0.603$  (○). (—) Best fit by Eq. (1) with  $\phi_\infty = 0.74$  and (□)  $B = 0.019$  and  $\tau = 55$  s, (◇)  $B = 0.027$  and  $\tau = 25$  s, (○)  $B = 0.037$  and  $\tau = 7$  s. The horizontal grey stripe corresponds to RCP.

### III. EXPERIMENTAL RESULTS

#### A. Continuous flow

Figure 3 displays the time evolution of the packing fraction  $\phi(t)$  of the granular bed when normalized by its initial value  $\phi_0$  for three upward continuous flow velocities,  $U_F/U_{Fc} = 0.4, 0.6$  and  $0.7$ , below the fluidization threshold. In each case  $\phi$  increases with time with thus a compaction of the granular bed by the weak upward flow. This means that an upward continuous flow below the minimum of fluidization leads continuously to local rearrangements that result in an increase of the solid fraction  $\phi$ . The compaction process is continuous during the long experiments that last typically a day, and no saturation that would lead to a final plateau value is seen. The compaction is higher for higher fluid velocity provided that the fluidization threshold is not overcome. For the highest possible flow rate  $U_F/U_{Fc} = 0.7$ , compaction is significant but rather slow as  $\phi$  increases by about 2% after one minute (from  $0.605$  up to about  $0.62$ ), by about 4% after one hour (up to  $\phi \simeq 0.63$ ) and by about 6% (up to  $\phi \simeq 0.645$ ) after one day. We have tested the two compaction laws reported in the introduction and have found that the one based on a stretched exponential (Eq. 2) does not fit well our data but the one based on a logarithm (Eq. 1) does. This is not surprising as our system is rather confined with only 10 bead diameters in the smallest dimension [3]. For each data series, the best fit is found for the maximal possible volume fraction  $\phi_\infty = 0.74$  but different values of the two other

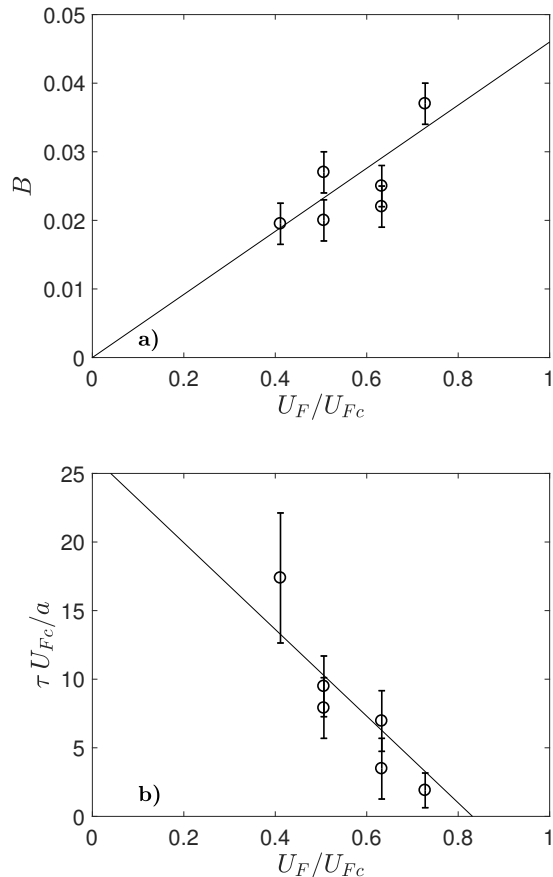


FIG. 4. a) Amplitude  $B$  and b) dimensionless characteristic time  $\tau U_{Fc}/a$  of the compaction dynamics by upward continuous flow as a function of the dimensionless flow velocity  $U_F/U_{Fc}$ . (o) Experimental data and (—) best linear fits.

parameters  $B$  and  $\tau$ . This means that in our compaction process the predicted final packing is the highest achievable one, even if our highest measured solid fraction was  $\phi \simeq 0.64$  for  $U_F/U_{Fc} \simeq 0.7$  after one day. The RZ law by which the solid fraction is related to the upward velocity for a fluidized bed for  $U_F > U_{Fc}$  seems thus no more valid for a bed packing for  $U_F < U_{Fc}$ . The values of the compaction efficiency  $B$  and of the characteristic time of compaction  $\tau$  when normalized by the characteristic settling time  $a/U_{Fc} \simeq 3$  s are shown in Fig. 4 as a function of the dimensionless upward velocity  $U_F/U_{Fc}$ . For increasing  $U_F/U_{Fc}$ ,  $B$  increases while  $\tau$  decreases, which means that compaction is stronger and quicker for larger  $U_F/U_{Fc}$  provided that  $U_F/U_{Fc} < 1$ . Note that we do not observe any significant dependence of  $B$  and  $\tau$  with  $\phi_0$ . Note also that it was not possible to perform experiments below  $U_F/U_{Fc} = 0.4$  because the pump does not deliver a continuous flow anymore at too low flow rates. In this limited flow range, the compaction time  $\tau$  appears to decrease with increasing  $U_F$  and a linear fit of the data leads to a vanishing  $\tau$  for  $U_F/U_{Fc} = 0.85 \pm 0.15$ , rather close to

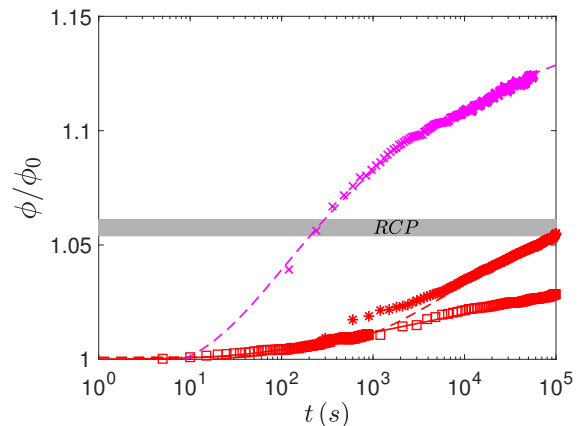


FIG. 5. Normalized solid fraction  $\phi/\phi_0$  as a function of time  $t$  for upward flow bursts of dimensionless velocity (\*)  $U_F/U_{Fc} = 0.4$  ( $T = 15$  s) and (x)  $U_F/U_{Fc} = 2.6$  ( $T = 11, 6$  s) corresponding to the same dimensionless flow displacement  $T_f U_F/a = 0.54$  with accordingly varying burst time duration  $T_f$ , and the same waiting time  $T_w = T - T_f = 11$  s. (---) Best fits by Eq. (1) with  $\phi_\infty = 0.74$  and with (\*)  $B = 0.07$  and  $\tau = 945$  s, and (x)  $B = 0.21$  and  $\tau = 37$  s. (□) Same data and fit as in Fig. 3 for continuous flow at  $U_F/U_{Fc} = 0.4$ . The horizontal thick grey line corresponds to RCP.

the value 1 corresponding to the experimental fluidization threshold. Note that at  $U_F/U_{Fc} \simeq 0.9$ , thus very close to the fluidization threshold, we observe some intermittency with successive irregular phases of compaction and decompaction. This behavior is not surprising and may be driven by some noise [26], and a similar intermittency with successive phase of mixing and segregation have been observed in fluidized beds with two grain sizes [27]. When the flow rate is significantly below the critical fluidization value ( $U_F < 0.9U_{Fc}$ ), we think that compaction arises from packing inhomogeneities that lead to permeability inhomogeneities and thus to flow inhomogeneities: some local zones of lower packing fractions (higher permeabilities) are submitted to higher upward flow rates above the critical one that lead to local fluidization with possible local rearrangements.

## B. Flow bursts

Let us now consider the effect of successive flow bursts. Our bursting experiments consist of a short flow time  $T_f$  followed by a long resting (no flow)  $T_w$  time before the next flow time, with thus the time period  $T = T_f + T_w$  as sketched in Fig. 1c. A constant upward velocity  $U_F$  is kept during each flow burst. The burst flow time  $T_f$  has been chosen such as the resulting fluid displacement is about one grain size,  $T_f \sim a/U_F$ , whereas the waiting time  $T_w$  has been chosen large enough for the grains to settle before the next flow burst, thus larger than the typical settling time  $a/U_{Fc} \sim 3$  s. In practice,  $T_w$

is kept constant with the large enough value  $T_w = 11$  s whereas  $T_f$  is adjusted with the  $U_F$  value in the range  $0.5 \lesssim T_f \lesssim 4$  s. Figure 5 displays the time evolution of the normalized solid fraction  $\phi(t)/\phi_0$  for two burst experiments with flow velocity below ( $U_F/U_{Fc} = 0.4$ ) and above ( $U_F/U_{Fc} = 2.6$ ) the critical fluidization velocity together with the continuous experiments of Fig. 3 corresponding to the same flow velocity below threshold. Two amazing facts arise from the results. The first amazing thing is that burst flow leads to a much more efficient compaction than continuous flow at the same value ( $U_F/U_{Fc} = 0.4$ ) below the threshold of fluidization. Indeed, after one day experiments corresponding here to about  $N = t/T \simeq 6 \times 10^3$  flow bursts, the increase is of about 5%, whereas the increase is less than 3% by continuous flow. Burst flow is even more efficient for compaction when considering the injected fluid amount which is reduced by the factor  $T_f/T \simeq 0.27$  when compared to continuous flow. The second amazing thing is that compaction is still observed for flow bursts above the threshold of fluidization and that the resulting compaction is much more efficient than the one below. Indeed, after one day the compaction is of about 12% at  $U_F/U_{Fc} = 2.6$  (see Fig. 5), thus 2.5 times higher than at  $U_F/U_{Fc} = 0.4$ . In that case, the bed solid fraction is observed to be above the random close packing value as  $\phi_{RCP} \simeq 0.64$  is reached after about only 4 minutes corresponding to only  $N \simeq 20$  flow bursts, and  $\phi \simeq 0.68$  is reached after about one day experiment ( $N \simeq 7 \times 10^3$ ). At such high solid fraction there should be some local crystallisation as reported recently in compaction by periodic shear [11].

The detailed action of the flow bursts is shown in Fig. 6 where the time evolution of the top position of the packing  $h$  relative to its initial value  $h_0$  and made dimensionless by the bead radius  $a$ ,  $(h - h_0)/a$ , is plotted for a few first burst periods. When the burst flow velocity  $U_F$  is above the critical fluidization velocity  $U_{Fc}$ , the packing is slightly fluidized during each flow burst with a small decompaction of about  $0.1a$  before a much larger compaction during the rest time  $T_w$ . By contrast, when the burst flow velocity is below the critical fluidization velocity ( $U_F < U_{Fc}$ ), there is no fluidization as expected but a slow and about continuous compaction.

By fitting the  $\phi(t)$  data points of Fig. 5 obtained by flow bursts by the same logarithmic law as for continuous flows (Eq. 1), we can extract the three parameters  $\phi_\infty$ ,  $B$  and  $\tau$ . As for the packing compaction by a weak continuous flow, best fits of data series for burst flows lead always to the highest possible value for the ultimate solid fraction:  $\phi_\infty = 0.74$ . The values of the two other parameters  $B$  and  $\tau$  when normalized by the typical settling time  $a/U_{Fc}$  are plotted in Fig. 7 as a function of the dimensionless burst flow velocity  $U_F/U_{Fc}$ . We observe that  $B$  increases and  $\tau$  decreases when  $U_F$  increases below the critical fluidization velocity ( $U_F/U_{Fc} < 1$ ) as for the continuous flow (Fig. 4). The  $B$  and  $\tau$  values for compaction by flow bursts are

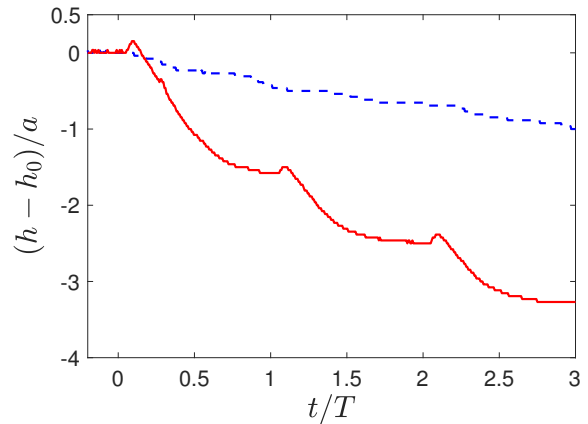


FIG. 6. Time evolution of the top position  $h$  of the packing relative to its initial value  $h_0$  made dimensionless by the bead radius  $a$  during a few first flow bursts for a burst flow velocity  $U_F$  below (---),  $U_F/U_{Fc} = 0.6$ ,  $T_f/T = 0.26$ ) and above (—),  $U_F/U_{Fc} = 2.6$ ,  $T_f/T = 0.08$ ) the fluidization threshold  $U_{Fc}$ . The waiting time  $T_w = 11$  s has been kept constant whereas the flow time  $T_f$  has been varied to keep constant the fluid displacement  $T_f U_F$ .

however quite different from the ones by continuous flow. Indeed,  $B$  and  $\tau U_{Fc}/a$  are about 4 times larger, but the effect of a larger  $B$  seems to be more important than the effect of a larger  $\tau$  so that the compaction dynamics by flow bursts is larger than by continuous flow. Above the critical fluidization velocity ( $U_F/U_{Fc} > 1$ ), the compaction efficiency parameter seems to saturate at a high plateau value  $B \simeq 0.2$ , whereas the characteristic time  $\tau$  is very low ( $\tau U_{Fc}/a < 3$ ). When looking at the characteristic number of bursts  $N_c = \tau/T$  (see inset of Fig. 6b),  $N_c$  decreases quite abruptly from about 60 when  $U_F/U_{Fc} < 1$  to  $N_c = 5 \pm 1$  when  $U_F/U_{Fc} > 1$ . This almost constant value may be due to the fact that the burst time  $T_f$  has been adjusted to the  $U_F$  value, such as the fluid displacement is the same and corresponds to about one grain size:  $T_f \simeq a/U_F$ .

#### IV. CONCLUSION

We have tested the possible compaction of liquid immersed granular packings, initially prepared by settling, from either continuous or bursting upward flow at low Reynolds number. The time evolution of the packing fraction was shown to follow a logarithmic evolution with three parameters corresponding to the ultimate solid packing, the compaction efficiency and the characteristic time. We have shown that compaction is possible with a continuous upward flow below the fluidization threshold, and that this compaction is stronger and faster close to this threshold. In this regime where the grains are no more in suspension but form a dense packing with

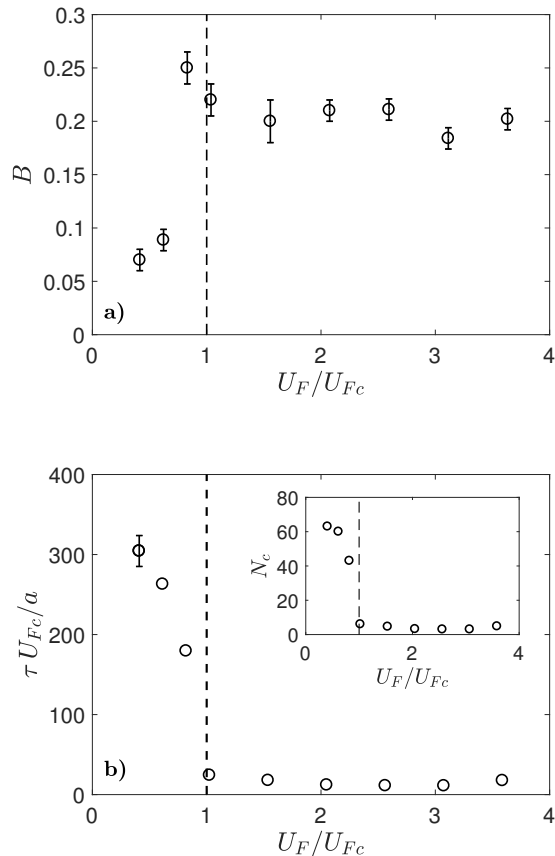


FIG. 7. a) Compaction amplitude  $B$  and b) dimensionless characteristic time  $\tau U_{Fc}/a$  of the compaction dynamics as a function of the dimensionless flow velocity  $U_F/U_{Fc}$  with the same fluid displacement during flow burst  $T_f U_F/a = 0.5$ . Inset: Corresponding characteristic number of bursts  $N_c = \tau U_{Fc}/a$  as a function of  $U_F/U_{Fc}$ .

permanent contact, the usual law of Richardson and Zaki (RZ) that relates the solid fraction to the upward fluid velocity for fluidized suspensions seems no more valid. Indeed, the observed logarithmic compaction process seems to go beyond the predicted RZ value for the solid fraction. A key point is that the compaction is even more efficient when the continuous flow is replaced by flow bursts. An even stronger and faster compaction is observed when the flow bursts are above the fluidization threshold, and seems to be the same when changing the flow rate but keeping constant the resulting fluid displacement for each burst flow (about one grain size). Complementary experiments should now be performed to explore the effect of the fluid displacement during each burst and to investigate the particle motions that lead to progressive compaction. An interesting point to investigate further would be the evolution of the packing state related to the different critical transitions [28] such as the glass transition, the jamming transition and the intermediate Gardner transition [29] recently observed experimentally in granular media [30].

## ACKNOWLEDGEMENTS

We thank A. Aubertin, L. Auffray and R. Pidoux for the building of the experimental set-up and A. Tariot for preliminary experiments. We acknowledge D. Salin, J. Martin, M. Nicolas and M. Schröter for stimulating discussions.

- 
- [1] J. B. Knight, C. G. Fandrich, C. N. Lau, H. M. Jaeger, and S. R. Nagel, *Physical review E* **51**, 3957 (1995).
  - [2] E. R. Nowak, J. B. Knight, E. Ben-Naim, H. M. Jaeger, and S. R. Nagel, *Phys. Rev. E* **57**, 1971 (1998).
  - [3] P. Philippe and D. Bideau, *EPL (Europhysics Letters)* **60**, 677 (2002).
  - [4] P. Richard, M. Nicodemi, R. Delannay, P. Ribiere, and D. Bideau, *Nat Mater* **4**, 121 (2005).
  - [5] P. Ribière, P. Richard, P. Philippe, D. Bideau, and R. Delannay, *The European Physical Journal E* **22**, 249 (2007).
  - [6] J. A. Dijksman and M. van Hecke, *EPL (Europhysics Letters)* **88**, 44001 (2009).
  - [7] P. Richard, P. Philippe, F. Barbe, S. Bourlès, X. Thibault, and D. Bideau, *Physical Review E* **68**, 020301 (2003).
  - [8] T. Bouteux and P. de Gennes, *Physica A: Statistical Mechanics and its Applications* **244**, 59 (1997).
  - [9] E. Ben-Naim, J. Knight, E. Nowak, H. Jaeger, and S. Nagel, *Physica D: Nonlinear Phenomena* **123**, 380 (1998).
  - [10] O. Pouliquen, M. Belzons, and M. Nicolas, *Phys. Rev. Lett.* **91**, 014301 (2003).
  - [11] F. Rietz, C. Radin, H. L. Swinney, and M. Schröter, *Phys. Rev. Lett.* **120**, 055701 (2018).
  - [12] J.-E. Mathonnet, P. Sornay, M. Nicolas, and B. Dalloz-Dubrujeaud, *Physical Review E* **95**, 042904 (2017).
  - [13] G. Onoda and E. Liniger, *Phys. Rev. Lett.* **64**, 2727 (1990).
  - [14] G. R. Farrell, K. M. Martini, and N. Menon, *Soft Matter* **6**, 2925 (2010).
  - [15] M. Schröter, D. I. Goldman, and H. L. Swinney, *Phys. Rev. E* **71**, 030301 (2005).
  - [16] C. Lesaffre, V. Mineau, D. Picart, and H. Van Damme, *Comptes Rendus de l'Académie des Sciences-Series IV-Physics* **1**, 647 (2000).

- [17] S. Kiesgen de Richter, C. Hanotin, P. Marchal, S. Leclerc, F. Demeurie, and N. Louvet, *The European Physical Journal E* **38**, 74 (2015).
- [18] A. Amon, R. Bertoni, and J. Crassous, *Physical Review E* **87**, 012204 (2013).
- [19] N. Gravish and D. I. Goldman, *Physical Review E* **90**, 032202 (2014).
- [20] J. Soundar, N. Vandenberghe, and Y. Forterre, *Physical review letters* **117**, 098003 (2016).
- [21] C. Li, P. B. Umbanhowar, H. Komsuoglu, D. E. Koditschek, and D. I. Goldman, *Proceedings of the National Academy of Sciences* **106**, 3029 (2009).
- [22] G. G. Jpseph, R. Zenit, M. L. Hunt, and A. M. Rosenwinkel, *Journal of Fluid Mechanics* **433**, 329 (2001).
- [23] P. Gondret, M. Lance, and L. Petit, *Physics of Fluids* **14**, 643 (2002).
- [24] J. Richardson and W. Zaki, *Trans. Instn. Chem. Engrs.* **32** (1954).
- [25] J. Martin, N. Rakotomala, and D. Salin, *Phys. Fluids* **7**, 2510 (1995).
- [26] R. Fischer, P. Gondret, and M. Rabaud, *Phys. Rev. Lett.* **103**, 128002 (2009).
- [27] A. Deboeuf, G. Gauthier, J. Martin, and D. Salin, *New Journal of Physics* **13**, 075005 (2011).
- [28] D. I. Goldman and H. L. Swinney, *Phys. Rev. Lett.* **96**, 145702 (2006).
- [29] L. Berthier, P. Charbonneau, Y. Jin, G. Parisi, B. Seoane, and F. Zamponi, *Proceedings of the National Academy of Sciences* **113**, 8397 (2016), <https://www.pnas.org/content/113/30/8397.full.pdf>.
- [30] A. Seguin and O. Dauchot, *Phys. Rev. Lett.* **117**, 228001 (2016).